Original Article

MST1 enhances radio-sensitivity in glioblastoma by suppressing autophagy and promoting apoptosis

Fangping Zhong*, Nan Zhang*, Yuheng Wang, Xuzhi He, Binfeng Tu

Department of Neurosurgery, Daping Hospital, Army Medical University, Chongqing 400042, China. *Equal contributors and co-first authors.

Received April 18, 2025; Accepted September 19, 2025; Epub September 25, 2025; Published September 30, 2025

Abstract: Resistance to radiotherapy remains a significant challenge in the treatment of glioblastoma (GBM). However, the mechanism underlying radioresistance in GBM cells are not fully elucidated. Autophagy has been implicated in supporting cancer cell growth and contributing to therapeutic resistance. Mammalian Ste20-like kinase 1 (MST1) exhibits variable expression patterns across a range of neoplasms, yet its role in modulating GBM radiosensitivity remains unclear. Analysis of The Cancer Genome Atlas (TCGA) disclosed that the correlation between MST1 level and patient survival varied across different cancer types. Notably, MST1 expression was decreased in the majority of tumors examined, including GBM, compared with normal tissue. A radiation-resistant GBM cell line (U87-IR) was established through sequential irradiation and observed significant downregulation of MST1 in U87-IR cells. Overexpression of MST1 increased the production of radiation-induced reactive oxygen species (ROS), impaired mitochondrial function, and promoted apoptosis by suppressing autophagy. Collectively, these results suggest that reduced MST1 expression enhances the survival of radiation-exposed GBM cells. Overexpression of MST1 inhibits autophagy and promotes apoptosis, thus enhancing the radio-sensitivity of GBM.

Keywords: MST1, radiotherapy resistance, glioblastoma, autophagy, apoptosis

Introduction

Glioblastoma (GBM) is a malignant tumor of the brain [1]. GBM is highly invasive and infiltrative, often involving critical functional brain regions, which makes complete surgical resection difficult and contributes to the poor prognosis [2, 3]. Current standard treatment strategies for GBM primarily consists of surgery followed by adjuvant treatments, including radiotherapy and chemotherapy [4]. Radiotherapy remains a key component of adjuvant therapy. However, the intrinsic biological characteristics of GBM cells and the tumor environment confer low radiosensitivity in most patients [5]. Moreover, GBM frequently acquires resistance and relapse during radiotherapy, posing a major challenge to effective disease management.

The exposure of cells to radiation results in severe deoxyribonucleic acid (DNA) damage and cell death. Radiation-induced DNA ionization or production of reactive oxygen species

(ROS) leads to DNA damage [6]. To maintain genome stability during DNA damage, cells activate two primary pathways for double-strand break (DSB) repair: non-homologous end-joining (c-NHEJ) and homologous recombination (HR), both of which are essential for the DNA damage response (DDR) [7]. Following irradiation, cells undergo apoptosis if DNA damage is beyond repair [8].

Mitochondria are pivotal in cancer progression, acting as the primary energy sources. Accumulating evidence has revealed that mitochondria supply the energy required for DDR after radiation [9, 10]. However, persistent low-level radiation exposure can elevate mitochondrial ROS, disrupt cell-cycle regulation via protein oxidation, and induce genomic instability [11].

Mammalian Ste20-like kinase 1 (MST1) promotes apoptosis by inhibiting autophagy [12]. Recent studies have demonstrated that MST1 reduces cell viability and induces apoptosis in

GBM cells [13] and regulates GBM cell growth through the Akt/mTOR signaling cascade [14]. Nevertheless, the role of MST1 in the GBM radioresistance remains unclear. This study aims to elucidate the molecular basis by which MST1 regulates radioresistance in GBM, hoping to provide potential strategies for targeted radiotherapy.

Materials and methods

Cell culture and irradiation

The U87 cell line is one the most extensively utilized and well-characterized GNM models, exhibiting key features of GBM such as rapid proliferation, strong invasiveness, and resistance to apoptosis. Therefore, it was selected for this study. The U87 cells were obtained from the American Type Culture Collection (ATCC) and cultured in Dulbecco's Modified Eagle Medium (DMEM) (Gibco) supplemented with 10% fetal bovine serum (FBS; Gibco). Cultures were maintained at 37°C in a humidified atmosphere containing 5% CO₂. U87 cells were cultivated in 60 mm culture dishes and subjected to 2 Gy using a 60Co γ-ray source. To establish a radioresistant GBM cell line (U87-IR), the U87 cells were seeded at 5×10³ cells per dish and treated with 2 Gy radiation followed by a 24 h recovery phase. This cycle was repeated 40 times, accumulating a total radiation dose of 80 Gy, as previously described [15].

Western blot

Cellular proteins were extracted using RIPA buffer (Beyotime, China). Protein concentration was quantified, and 20 μg of protein per sample was separated on sodium dodecyl sulfate - polyacrylamide gel (SDS-PAGE) and transferred to polyvinylidene fluoride (PVDF) membranes (Millipore, Billerica, MA, USA). Membranes were blocked 5% bovine serum albumin (BSA) and then incubated with primary antibodies overnight at 4°C, followed by incubation with secondary antibodies for 1 h at room temperature.

The primary antibodies included β -actin (dilution rate 1:5000, product ID 3700), cleaved caspase-3 (1:2000, 9664), cleaved caspase-9 (1:2000, 9509) (Cell Signaling Technology, USA); MST1 (1:2000, ab245190), SIRT6

(1:3000, ab191385), HSP60 (1:2500, ab-190828), LC3B (1:2000, ab192890), Bax (1:2000, ab32503), and p62 (1:3000, ab-109012) (Abcam, UK). The secondary antibodies included IgG-HRP (1:100, goat anti-rabbit), IgG-HRP (1:1000, goat anti-rabbit, ab1987), and IgG-HRP (1:1500, goat anti-mouse, ab19235) (Abcam, UK).

Immunoblot bands were visualized and quantified using ImageJ version 1.51p. Protein expression levels normalized to β -actin and presented as relative fold changes.

Subcutaneous tumor model in nude mice

Male BALB/c nude mice (6-8 weeks old) were sourced from the Animal Experiment Center of Guangxi Medical University. The mice were housed under controlled conditions ($23 \pm 2^{\circ}$ C, $50 \pm 5\%$ humidity, and a 10/14-hour light/dark cycle). All animal procedures were approved by the Animal Care and Ethics Committee of Guangxi Medical University (AMUWEC2025-7049).

Lentiviral vectors carrying MST1 were produced by GenePharma (China). MST1-overexpresing U87 cells were selected using Puromycin (2.5 µg/ml). For tumor implantation, U87 cells (1×10⁷) either overexpressing MST1 or serving as controls were suspended in 200 µL of DMEM and then administered via subcutaneous injection into the right flanks of mice. The implanted tumor was locally irradiated with 5 Gy, and the tumor volumes were assessed every four days post-irradiation. On day 25 after implantation, mice were euthanized using isoflurane, and the tumors were excised, weighed, and photographed. The tumor size was calculated using the formula: V (mm³) = $1/6 \pi \times \text{length (mm)} \times \text{width}^2 \text{ (mm}^2).$

Transfection

For cell transfection experiments, cells were transfected with plasmids or small interfering ribonucleic acids (siRNAs) using Effectene Transfection Reagent (Qiagen GmbH). To achieve MST1 overexpression, the MST1 coding sequence was cloned into the pcDNA6.0 vector (pcDNA-MST1 construct). For MST1 and SIRT6 knockdown, siRNAs were sourced from Sangon Biotech (Shanghai, China). To inhibit autophagy, U87 cells were exposed to a con-

centration of 1.25 mM 3-methyladenine (3-MA, M9281, Sigma Aldrich).

Flow cytometric analysis

Mitochondrial membrane potential (MMP) was assessed using the Mitochondrial Membrane Potential Assay Kit (Cell Signaling, USA). Following the designated treatment, cells were incubated with the membrane-permeant JC-1 dye for 45 min at 37°C and then analyzed by flow cytometry.

The production of reactive oxygen species (ROS) was evaluated using a ROS assay kit (Solarbio, China). In brief, cells were incubated at 37°C for 24 h and then stained with 10 μM DCFH-DA for 15 min in the dark. Subsequently, the stained cells were subjected to flow cytometric analysis using equipment from BD Biosciences.

In the case of apoptosis assessment, the collected cells were treated with a combination of annexin V (10 $\mu L)$ and propidium iodide (10 μL , Solarbio, China) for 30 minutes at room temperature. After centrifugation at 600×g for 3 minutes, the cells were subjected to flow cytometric examination.

Cell viability assays

Cell viability was evaluated using an MTT assay kit (Solarbio, China). Cells were seeded in 96-well plates to 75% confluence and treated as indicated. MTT solution (5 mg/mL) was added to each well and incubated for 4 hours at 37°C. The supernatant was then removed, and 50 μ l of DMSO was added to dissolve formazan crystals. Absorbance was measured at 490 nm to determine cell viability.

Data collection and analysis

RNA-seq data for 33 cancer types (**Table 1**) were retrieved from The Cancer Genome Atlas (TCGA) and Genotype-Tissue Expression (GTEx) databases. Differential MST1 expression between tumor and normal tissues was analyzed using the Wilcoxon test. MST1 protein levels in tumors were examined via the Human Protein Atlas (HPA) and its subcellular localization was confirmed by immunofluorescence microscopy.

Clinical data for these cancers were sourced from TCGA, and overall survival (OS) was used to assess the prognostic value of MST1 expression. Samples were divided into high- and low-expression groups based on the median MST1 value. Kaplan-Meier survival curves and Cox regression analyses were performed using R packages "survminer" and "survival", with results visualized in forest plots.

Microarray data for glioblastoma (GSE188256) were obtained from the GEO database. The extracted data were log2-transformed for normalized using the quantile normalization function in the R software "preprocessCore" package (version 3.4.1). The cBioPortal web platform (https://www.cbioportal.org/) was used to analyze the genomic alterations of MST1, including mutations, amplifications, and deep deletions, which were used to analyze pan-cancer mutation frequencies.

Statistical analysis

All experiments were repeated three times. Data were expressed as mean \pm standard deviation (SD). The experimental data were statistically analyzed utilizing the SPSS software (version 22.0; IBM Corp.). Comparisons among multiple groups were conducted using oneway analysis of variance (ANOVA) followed by Tukey's post hoc test. The two groups were compared using t-test. The Kaplan-Meier survival analysis comparison was conducted using logrank test. For analyses involving multiple time points, repeated-measures ANOVA was used. A P value <0.05 was considered statistically significant.

Results

Comprehensive analysis of MST1 in pan-cancer: expression, survival impact, and genetic alterations

The association between MST1 expression and overall survival (OS) across various cancers was initially evaluated using TCGA data. Elevated MST1 levels were correlated with poor OS in patients with kidney chromophobe (KICH) and pheochromocytoma/paraganglioma (PCPG), whereas higher MST1 expression was associated with improved OS in patients with kidney renal papillary cell carcinoma

Table 1. The abbreviations and corresponding full names of 33 cancers

| Cancer Type | Abbreviation |
|--|--------------|
| adrenocortical carcinoma | ACC |
| bladder urothelial carcinoma | BLCA |
| breast invasive carcinoma | BRCA |
| cervical squamous cell carcinoma and endocervical adenocarcinoma | CESC |
| cholangiocarcinoma | CHOL |
| colon adenocarcinoma | COAD |
| ymphoid neoplasm diffuse Large B-cell lymphoma | DLBC |
| esophageal carcinoma | ESCA |
| glioblastoma multiforme | GBM |
| nead and neck squamous cell carcinoma | HNSC |
| kidney chromophobe | KICH |
| kidney renal clear cell carcinoma | KIRC |
| kidney renal papillary cell carcinoma | KIRP |
| acute myeloid leukemia | LAML |
| orain lower grade glioma | LGG |
| iver hepatocellular carcinoma | LIHC |
| ung adenocarcinoma | LUAD |
| ung squamous cell carcinoma | LUSC |
| mesothelioma | MESO |
| ovarian serous cystadenocarcinoma | OV |
| pancreatic adenocarcinoma | PAAD |
| pheochromocytoma and paraganglioma | PCPG |
| prostate adenocarcinoma | PRAD |
| ectum adenocarcinoma | READ |
| sarcoma | SARC |
| skin cutaneous melanoma | SKCM |
| stomach adenocarcinoma | STAD |
| esticular germ cell tumors | TGCT |
| hyroid carcinoma | THCA |
| hymoma | THYM |
| uterine corpus endometrial carcinoma | UCEC |
| uterine carcinosarcoma | UCS |
| uveal melanoma | UVM |

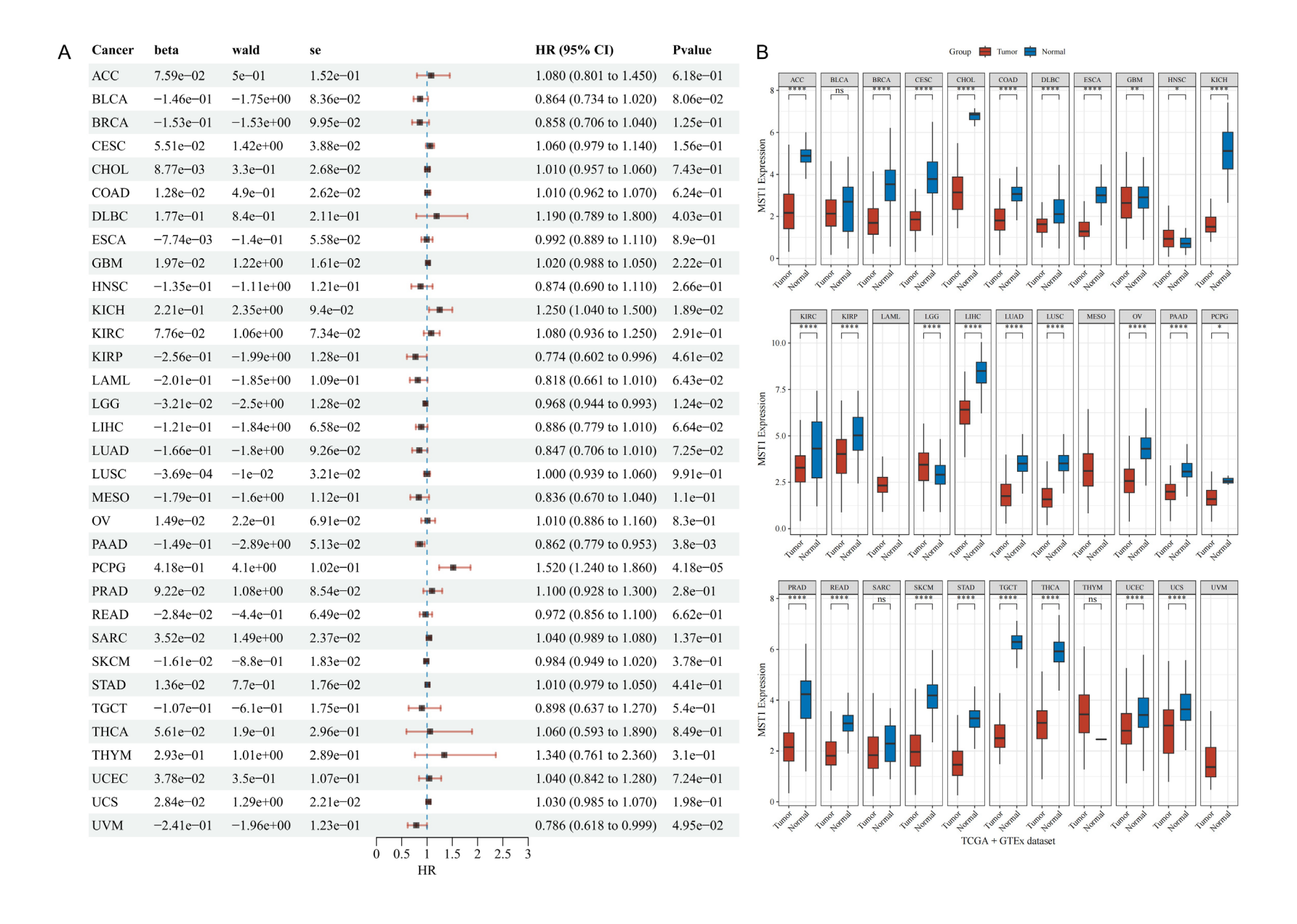
(KIRP), lower-grade glioma (LGG), pancreatic adenocarcinoma (PAAD), and uveal melanoma (UVM) (**Figure 1A**).

MST1 expression in 33 tumor types was assessed by combining the TCGA and GTEx datasets. MST1 level was decreased in 25 cancers compared with normal tissues, whereas head and neck squamous cell carcinoma (HNSC) and LGG exhibited increased expression (Figure 1B). Validation using the GSE-188256 dataset from GEO confirmed that MST1 mRNA levels were lower in GBM tissues

than in adjacent non-tumor samples (**Figure 1C**).

Immunofluorescence data from the HPA revealed MST1 subcellular localization in HeLa, HepG2, and U2OS cells was predominantly distributed in cytoplasmic vesicles (**Figure 1D**).

Genomic alterations of MST1 across cancers were further examined using cBioPortal. Diffuse large B-cell lymphoma (DLBC) displayed the highest frequency of genetic changes (8.26%), predominantly deep deletions. In GBM, muta-



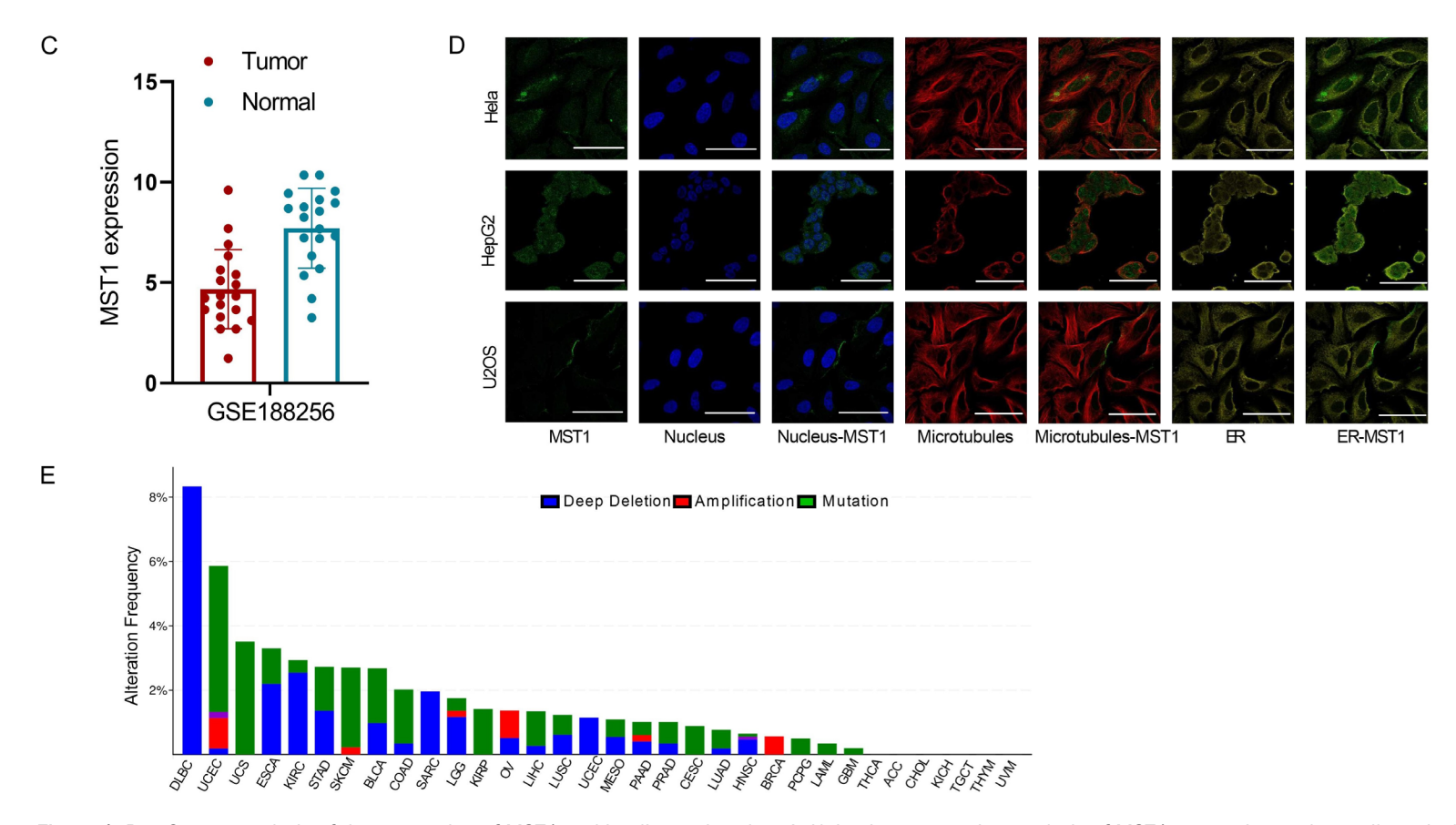


Figure 1. Pan-Cancer analysis of the expression of MST1 and its diagnosis value. A. Univariate regression analysis of MST1 expression and overall survival across 33 cancer types. B. MST1 expression in tumor versus normal tissues from pan-cancer analysis. C. MST1 expression in tumor and normal tissues in glioblastoma (GBM) from GSE188256 (19 human glioma tissues and corresponding adjacent non-tumor tissues). D. Immunofluorescence staining of the subcellular localization of MST1 in The Human Protein Atlas database. Scale bar: 50 μm. Magnification: 20×. E. Genetic alterations of MST1 in pan-cancer analysis using the cBioPortal. ^{ns}P>0.05; *P<0.05; *P<0.01; ****P<0.001.

tions constituted the primary form of MST1 alteration (Figure 1E). Collectively, these findings suggest that MST1 is downregulated in multiple human cancers, including GBM, and may serve as a potential prognostic indicator across tumor types.

MST1 decreases cell viability and promotes radiation-induced apoptosis of GBM

Next, the biological role of MST1 in GBM cells was investigated. MST1 overexpression was achieved by transfecting cells with the pcDNA-MST1 plasmid. MTT assay demonstrated that MST1 overexpression significantly reduced cell viability compared with control cells (Figure 2A). Flow cytometry demonstrated a higher proportion of apoptotic cells in the MST1overexpressing cells (Figure 2B). Furthermore. WB further showed that MST1 overexpression enhanced the expression of cleaved caspase-3 and caspase-9 in radiation-treated cells (Figure 2C). Consistently, flow cytometry confirmed that MST1 overexpression markedly promoted radiation-induced apoptosis (Figure 2D). Collectively, these findings indicated that MST1 promotes GBM cell death in response to radiation.

Overexpression of MST1 enhances radiationinduced mitochondrial damage

Mitochondrial impairment and endoplasmic reticulum (ER) stress are closely linked and jointly regulate apoptosis following radiation. Therefore, we tested the effects of MST1 on radiation-induced mitochondrial damage. As shown in Figure 3A, intracellular ROS levels in U87 cells increased after exposure to radiation, which was further enhanced by MST1 overexpression. Consistently, mitochondrial ATP contents decreased more significantly in MST1-overexpressed-cells following radiation (Figure 3B). Flow cytometric analysis of mitochondrial membrane potential (MMP) using JC-1 staining indicated that irradiation reduced the JC-1 red fluorescence, signifying depolarization of MMP, which was later attenuated by overexpression of MST1 (Figure 3C).

Aberrant mitochondrial unfolded protein response (UPR^{mt}) signaling has been implicated in radioresistance [16]. Exposure to radiation significantly enhanced the expression of HSP60, a

known UPR^{mt} marker protein, whereas MST1 overexpression suppressed this induction (**Figure 3D**).

Analysis of TCGA database demonstrated a significant increase in HSP60 levels in malignant tissues compared to normal tissue samples. Additionally, Kaplan-Meier method indicated that GBM patients with high HSP60 expression experienced a 54% increased risk of death compared to those with low expression (HR = 1.541; 95% confidence interval (CI): 1.194-1.989) (Figure 3E). Collectively, these data suggest that MST1 aggravates radiation-induced mitochondrial damage by affecting UPR^{mt} signaling.

MST1 enhances radio-sensitivity of GBM tumors

To validate the unique role of MST1 in modulating radio-resistance, a xenograft GBM model was established in nude mice through ectopic implantation. Tumors derived from U87 cells were exposed to localized irradiation, and growth was monitored. MST1 overexpression markedly enhanced radiotherapy response, as evidenced by reduced tumor volume and weight compared with controls (Figure 4A). We next investigated whether MST1-mediated radio-sensitization was dependent on SIRT6. Tumors derived from MST1-overexpressing cells exhibited significantly elevated SIRT6 levels (Figure 4B). Furthermore, MST1 overexpression increased the expression of cleaved caspase-3 and caspase-9; However, these proapoptotic effects were abolished when SIRT6 was silenced (Figure 4C). These data collectively indicate that MST1 promotes radiationinduced apoptosis through SIRT6 activation.

MST1 promotes radiation-induced apoptosis through suppressing autophagy

To further investigate the role of MST1 in radioresistance, a radioresistant GBM cell line (U87-IR) was established by subjecting U87 cells to repeated ionizing radiation, with a accumulative dose of 120 Gy over two weeks. Compared with parental cells, U87-IR cells exhibited reduced apoptosis after irradiation (**Figure 5A**), accompanied by decreased expression of cleaved caspase-3 and caspase-9 as well as lower MST1 expression (**Figure 5B**).

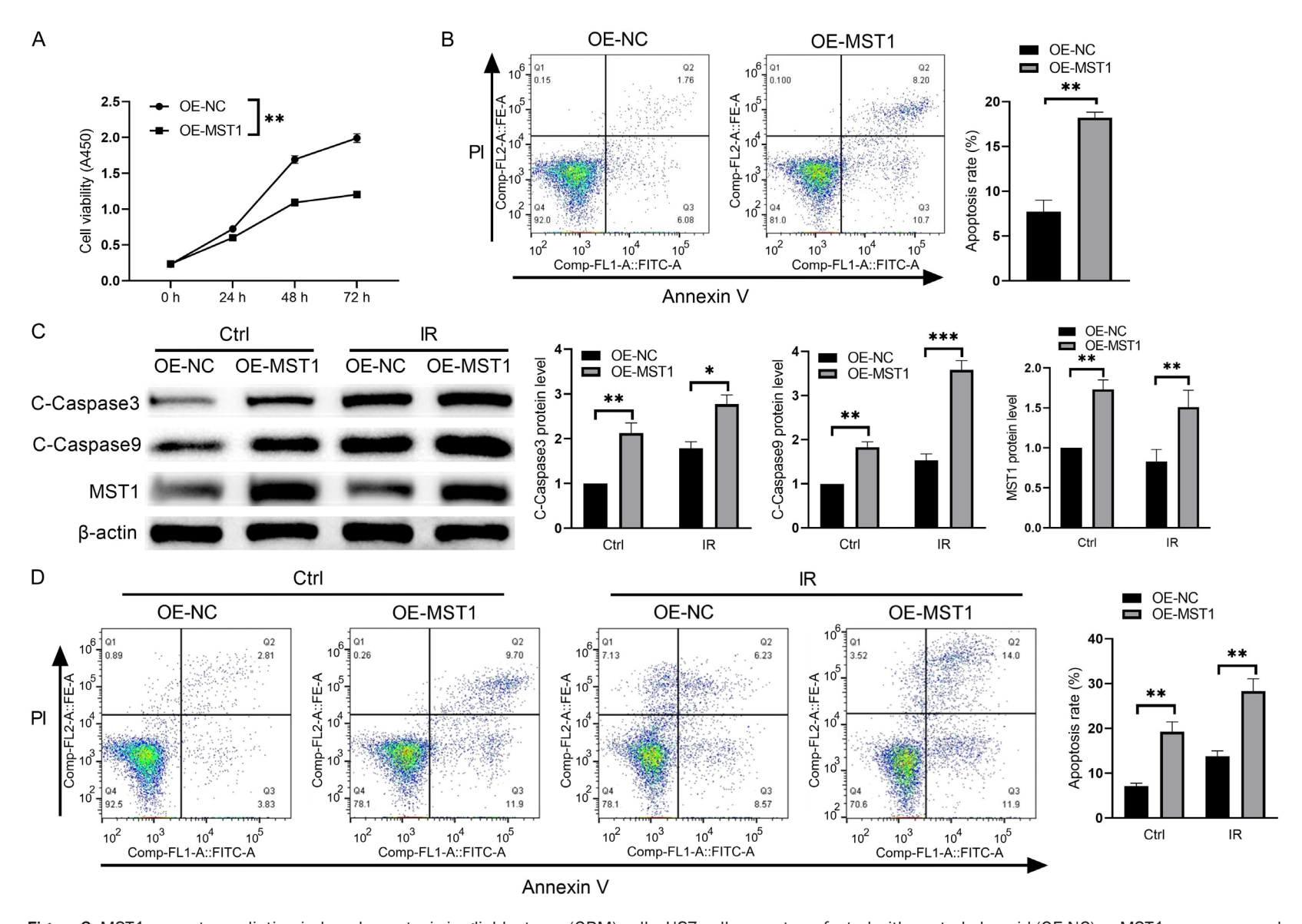


Figure 2. MST1 promotes radiation-induced apoptosis in glioblastoma (GBM) cells. U87 cells were transfected with control plasmid (OE-NC) or MST1-overexpressed plasmid (OE-MST1). A. Cell viability examined using the MTT assay. B. Flow cytometric analysis of apoptosis in U87 cells transfected with OE-NC or OE-MST1. C. Protein levels of cleaved-Caspase3 (C-Caspase3), cleaved-Caspase9 (C-Caspase9), and MST1 examined by western blot. D. Flow cytometric analysis of apoptosis in U87 cells transfected with OE-NC or OE-MST1 following irradiation. Data are presented as mean ± SD, n = 3. *P<0.05; **P<0.01.

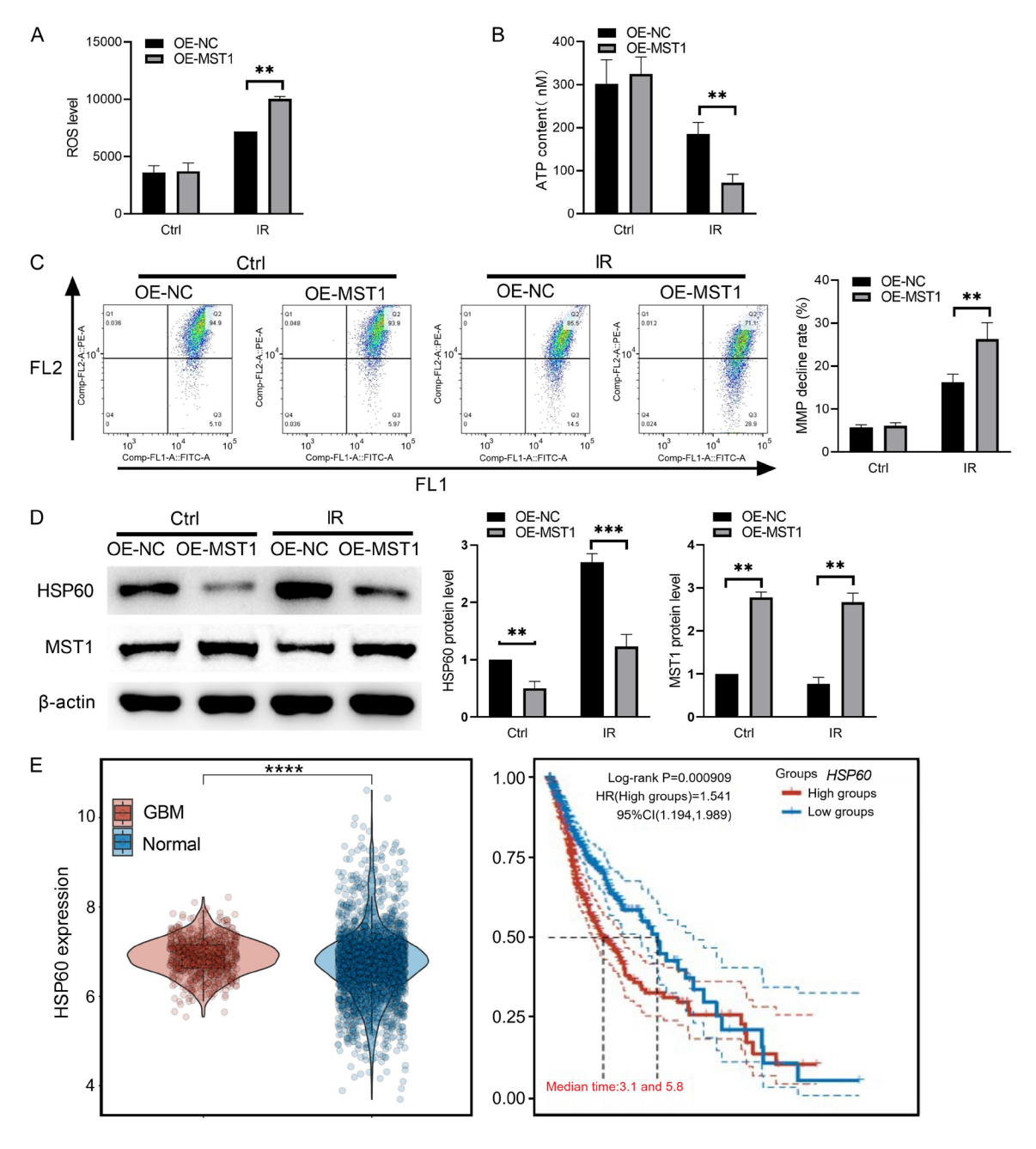


Figure 3. MST1 enhances radiation-induced mitochondrial damage in glioblastoma (GBM) cells. U87 cells were transfected with control plasmid (OE-NC) or MST1-overexpressed plasmid (OE-MST1), and then exposed to 5Gy irradiation. A. Intracellular reactive oxygen species (ROS) level. B. Intracellular adenosine triphosphate (ATP) level. C. Matrix metalloproteinase (MMP) was examined with JC-1 staining using flow cytometry. D. Protein levels of HSP60 and MST1 were examined by western blot. E. HSP60 expression in tumor tissues versus normal tissues from The Cancer Genome Atlas and Kaplan-Meier survival analysis of GBM patients stratified by HSP60 expression. Data are presented as mean \pm SD (n = 3). **P<0.01; ***P<0.001; ****P<0.0001.

Given the involvement of autophagy in radioresistance, we investigated whether MST1 regulates this process. MST1 overexpression in U87-IR cells reduced the ratio of LC3II/LC3I and increased p62 expression, indicating that MST1 inhibited autophagy (Figure 5C). Analysis of the TIMER2 database (http://timer.cistrome.org/) confirmed a negative correlation between MST1 and LC3 expression in GBM (Figure 5D). Moreover, MST1 Knockdown inhib-

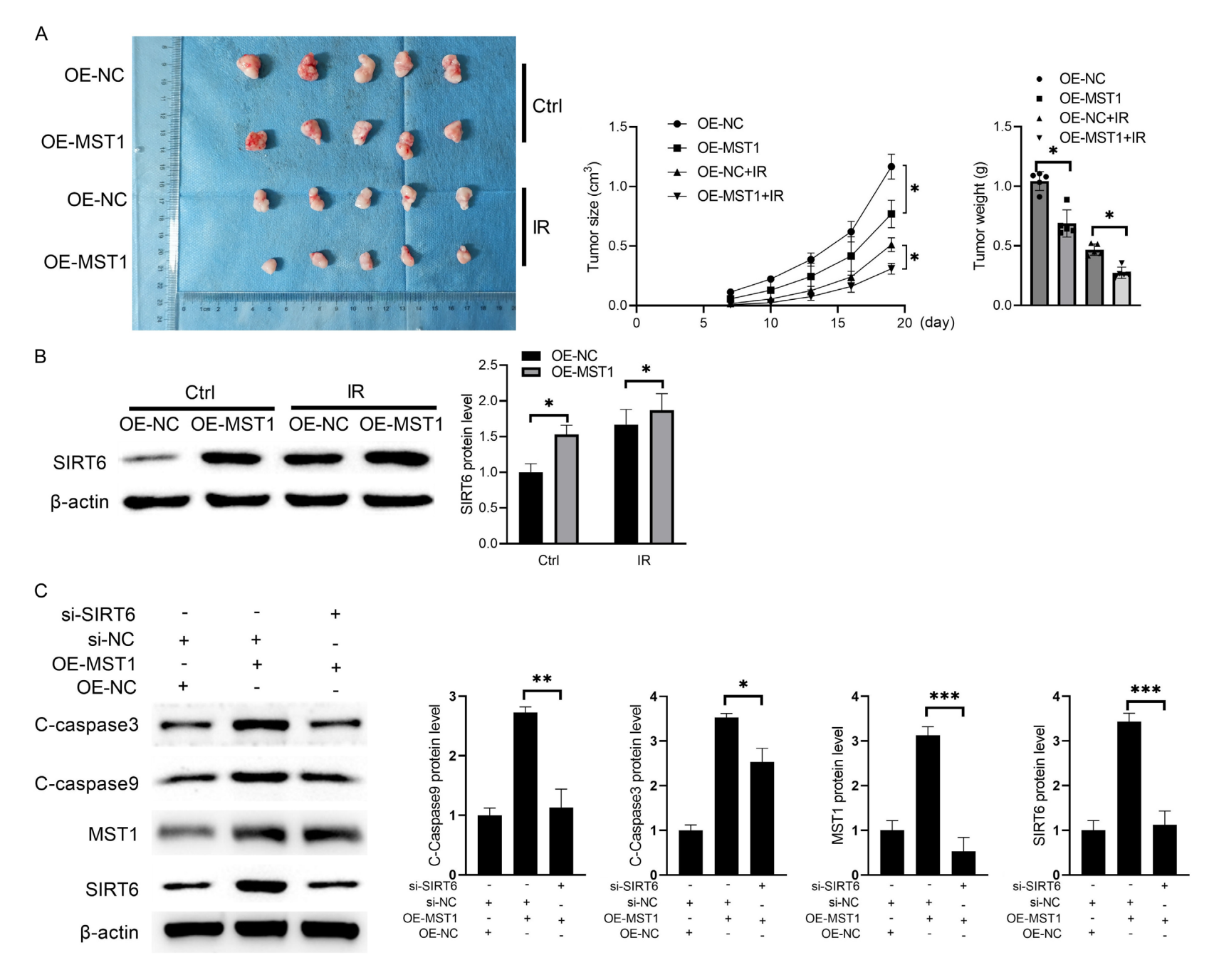


Figure 4. MST1 increases radio-sensitivity of glioblastoma (GBM) tumors. A. Tumor volumes. Data are presented as mean \pm SD from 5 mice per group. B. SIRT6 protein levels in xenograft tumors examined by western blot. C. U87 cells were transfected with si-NC, si-SIRT6, OE-NC, or OE-MST1 plasmids, and protein levels of cleaved-Caspase3 (C-Caspase3), cleaved-Caspase9 (C-Caspase9), SIRT6, and MST1 were detected by western blot. Data are presented as mean \pm SD (n = 3). *P<0.05; **P<0.01; ***P<0.001.

ited apoptosis by downregulating the pro-apoptotic protein Bax. However, this effect was attenuated by the autophagy inhibitor 3-MA (Figure 5E). Collectively, these results indicate that MST1 overexpression promotes radiation-induced apoptosis in GBM cells by inhibiting autophagy.

Discussion

Radioresistance is a major obstacle for effective GBM treatment. Hence, elucidating its underlying mechanisms may provide novel therapeutic strategies. Following irradiation, various cellular responses are activated, including DNA repair and apoptotic pathways [17]. In this study, we established a radioresistant GBM cell line (U87-IR) and observed significant downregulation of MST1 expression. MST1 has been implicated in multiple pathological processes. For example, MST1 inhibits pancreatic ductal adenocarcinoma development and progression by inducing pyroptosis [18]. In obesity-related nonalcoholic fatty liver disease, MST1 promotes hepatocyte mitochondrial apoptosis by regulating parkin-related mitophagy [19]. In addition, MST1 phosphorylates fork-head box 01/3 (Fox01/3) transcription factors to promote their nuclear translocation, thereby triggering neuronal cell death during ischemia-reperfusion injury [20]. TCGA data revealed that MST1 expression is variably associated with survival outcomes across cancers. Notably, MST1 is downregulated in most tumors, including GBM, and confirmed to be low in GBM tissues in the GSE188256 dataset. Genomic profiling further revealed varying frequencies and patterns of MST1 alterations across cancers, suggesting its potential utility as a prognostic marker.

Radiation activates the UPR^{mt} signaling pathway, which may function as a feedback mechanism in promoting cell survival [21]. The mitochondrial chaperone HSP60 helps restore protein homeostasis during mitochondrial stress [22]. In this study, MST1 overexpression suppressed HSP60, indicating that MST1 negatively regulates radiation-induced activation of

UPR^{mt} signaling. Kaplan-Meier survival analysis demonstrated that elevated HSP60 levels were associated with an unfavorable prognosis in GBM patients. Moreover, MST1 overexpression increased ROS production and promoted mitochondrial membrane potential loss, suggesting its role in modulating mitochondrial function under radiation stress.

In mammalian cells, MST1 normally acts as a proapoptotic molecule that facilitates cell death [23]. In some tumor cells, activation of SIRT6 has been reported to promote radiationinduced apoptosis [24]. In our research, MST1 overexpression in GBM cells enhanced caspase activation and apoptosis following radiation exposure. Mechanistically, MST1 promotes phosphorylation of FOXO3a, facilitating its dissociation and nuclear translocation to initiate SIRT6 gene transcription [13]. Consistent with this mechanism, silencing of SIRT6 attenuated MST1-induced cleavage of caspase-3 and -9. indicating that MST1 promotes radiationinduced apoptosis via SIRT6. Furthermore, in vivo experiment showed that tumors derived from MST1-overexpressing cells were more sensitive to radiation. In addition to pro-apoptotic functions, nuclear translocation of MST1 has been reported to inhibit microglial activation [25]. Evidence suggests that autophagy is induced in response to radiation exposure, yet its role in radioresistance remains controversial [26, 27]. Oxidative stress and unfolded protein responses signaling can stimulate autophagy, a key determinant of cellular survival after irradiation [28]. Conversely, rapamycin-induced autophagy sensitizes non-small cell lung carcinoma cells to radiation [29]. Literature regarding the role of autophagy in radioresistance remains inconsistent [30]. MST1 has been shown to suppress autophagy by phosphorylating Beclin1 and inducing homo-dimerization of Beclin1 [12]. Our experiments showed that overexpression of MST1 reduced the LC3II/LC3I ratio and increased p62 expression, whereas knockdown of MST1 had the opposite effect. Furthermore, suppression of autophagy using 3-MA mitigated the

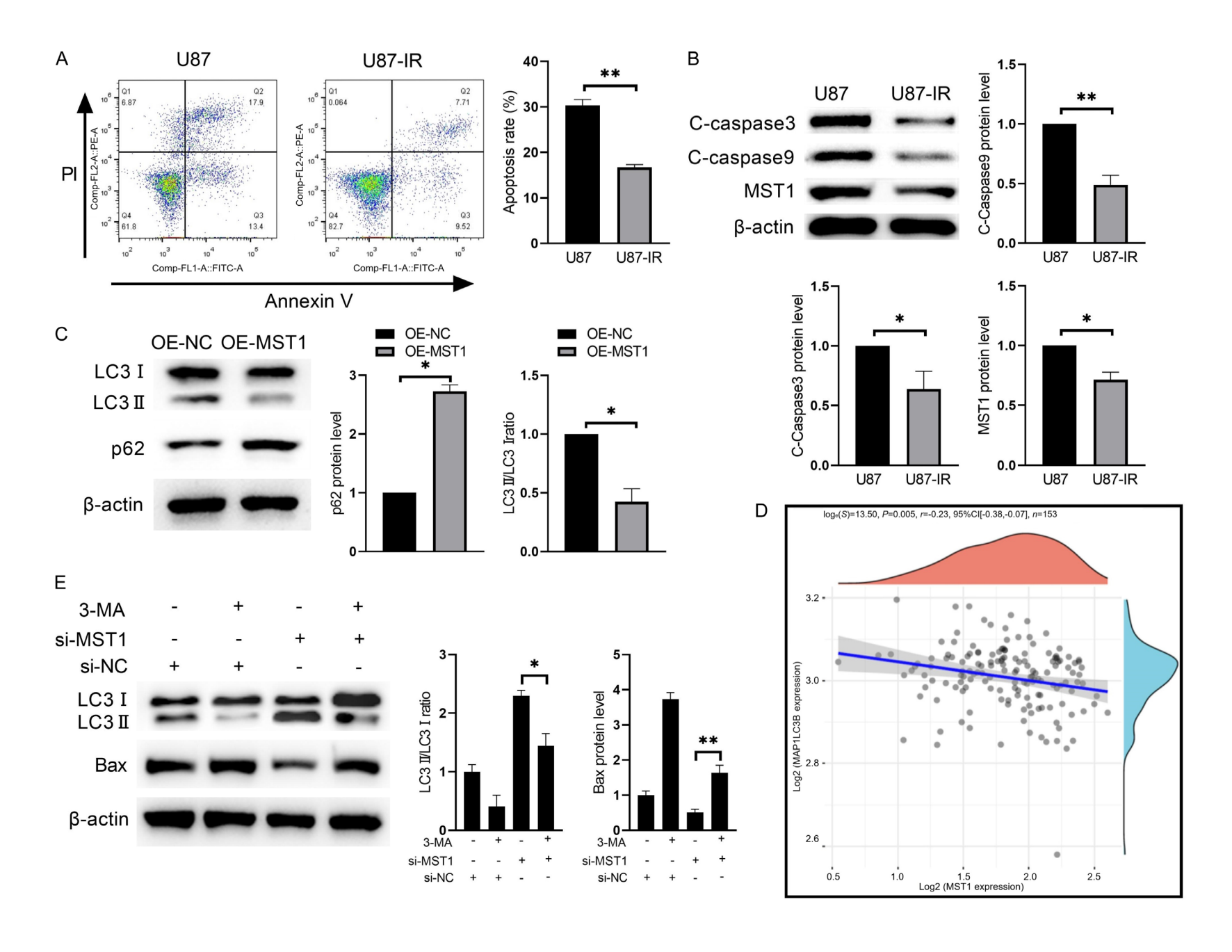


Figure 5. MST1 inhibits autophagy in glioblastoma (GBM) cells. A. Cell apoptosis in U87-IR and parental U87 cells examined by Annexin V/Pl staining. B. Protein levels of cleaved-Caspase3 (C-Caspase3), cleaved-Caspase9 (C-Caspase9), and MST1 in U87-IR and U87 cells examined by western blot. C. Protein levels of LC3 and p62 in U87-IR cells transfected with OE-NC or OE-MST1 examined by western blot. D. Correlation between MST1 and LC3 expression analyzed using Spearman's correlation analysis. The abscissa represents the expression distribution of the first gene, and the ordinate represents the expression distribution of the second gene. The density curve on the right represents the trend in distribution of the second gene, the upper density curve represents the trend in distribution of first gene expression. The value on the top represents the correlation p value, correlation coefficient and correlation calculation method. E. U87 cells transfected with si-NC or si-MST1 were treated with 3-MA (10 μ M, 45 min) before irradiation, and protein levels of Bax and LC3 were examined by western blot. Data are presented as mean \pm SD (n = 3). *P<0.05; **P<0.01.

reduction in apoptosis caused by MST1 knock-down. Collectively, these findings indicate that MST1 promotes radiation-induced apoptosis in GBM cells partially by suppressing autophagy.

Conclusion

MST1 expression is downregulated in radioresistant GBM cells and may serve as a potential prognostic biomarker. MST1 overexpression suppresses autophagy and modulates mitochondrial activity, thereby enhancing the radiosensitivity of GBM cells and promoting radiation-induced apoptosis. These findings underscore the potential of targeting MST1 to improve therapeutic outcomes in GBM radiotherapy.

Acknowledgements

This work has been supported by grants from Jiangxi Provincial Health Commission Project (No. 202130718).

Disclosure of conflict of interest

None.

Address correspondence to: Xuzhi He and Binfeng Tu, Department of Neurosurgery, Daping Hospital, Army Medical University, No. 10, Changjiang Branch Road, Daping, Yuzhong District, Chongqing 400042, China. Tel: +86-0791-88315120; Email: hxzh2024@tmmu.edu.cn (XZH); xiangyu163. tu@163.com (BFT)

References

- [1] Zou Y, Li S, Li Y, Zhang D, Zheng M and Shi B. Glioblastoma cell derived exosomes as a potent vaccine platform targeting primary brain cancers and brain metastases. ACS Nano 2025: 19: 17309-17322.
- [2] Stefan D, Lesueur P, Lequesne J, Feuvret L, Bronnimann C, Castéra M, Brachet PE, Hrab I, Ducloie M, Lacroix J, Lecornu M, Braux G,

- Christy F, Sunyach MP, Cohen-Jonathan Moyal E, Kao W, Faisant M, Emery E, Grellard JM, Sichel F, Laurent C, Fontanilles M and Clarisse B. Olaparib, temozolomide, and concomitant radiotherapy for partially resected or biopsy-only glioblastoma first-line treatment: results from the OLA-TMZ-RTE-01 Phase I study. Clin Cancer Res 2025; 31: 1212-1222.
- [3] Zhang L, Yang Y, Li Y, Wang C, Bian C, Wang H and Wang F. Epigenetic regulation of histone modifications in glioblastoma: recent advances and therapeutic insights. Biomark Res 2025; 13; 80.
- [4] Harwood DSL, Pedersen V, Bager NS, Schmidt AY, Stannius TO, Areškevičiūtė A, Josefsen K, Nørøxe DS, Scheie D, Rostalski H, Lü MJS, Locallo A, Lassen U, Bagger FO, Weischenfeldt J, Heiland DH, Vitting-Seerup K, Michaelsen SR and Kristensen BW. Glioblastoma cells increase expression of notch signaling and synaptic genes within infiltrated brain tissue. Nat Commun 2024; 15: 7857.
- [5] Liu X, Liu B, Wang J, Liu H, Wu J, Qi Y, Liu Y, Zhu H, Li C, Yang L, Song J, Yao G, Tian W, Zhao K, Han L, Shu K, Zhang S, Man J, You C, Huang H and Li R. PHGDH activation fuels glioblastoma progression and radioresistance via serine synthesis pathway. J Exp Clin Cancer Res 2025: 44: 99.
- [6] Peng H, Cui B, Wei J, Yuan M, Liu W, Shi J and Liu Y. Timosaponin AllI enhances radiosensitivity in breast cancer through induction of ROSmediated DNA damage and apoptosis. Radiat Res 2025; 203: 257-270.
- [7] Ceccaldi R, Rondinelli B and D'Andrea AD. Repair pathway choices and consequences at the double-strand break. Trends Cell Biol 2016; 26: 52-64.
- [8] Wang C, Zha YL, Wang H, Sun B, Qiang WG, Yuan Y, Shi HB and Hu WW. Carfilzomib promotes lodine-125 seed radiation-induced apoptosis, paraptosis, and ferroptosis in esophageal squamous cell carcinoma by aggravating endoplasmic reticulum stress. Transl Oncol 2025; 57: 102393.
- [9] Yu J, Wang Q, Chen N, Sun Y, Wang X, Wu L, Chen S, Yuan H, Xu A and Wang J. Mitochon-

- drial transcription factor A regulated ionizing radiation-induced mitochondrial biogenesis in human lung adenocarcinoma A549 cells. J Radiat Res 2013; 54: 998-1004.
- [10] Zhou Z, Jiang X, Yi L, Li C, Wang H, Xiong W, Li Z and Shen J. Mitochondria energy metabolism depression as novel adjuvant to sensitize radiotherapy and inhibit radiation induced-pulmonary fibrosis. Adv Sci (Weinh) 2024; 11: e2401394.
- [11] Shimura T, Sasatani M, Kawai H, Kamiya K, Kobayashi J, Komatsu K and Kunugita N. A comparison of radiation-induced mitochondrial damage between neural progenitor stem cells and differentiated cells. Cell Cycle 2017; 16: 565-573.
- [12] Ye H, Cai T, Shen Y, Zhao L, Zhang H, Yang J, Li F, Chen J and Shui X. MST1 knockdown inhibits osteoarthritis progression through Parkin-mediated mitophagy and Nrf2/NF-κB signalling pathway. J Cell Mol Med 2024; 28: e18476.
- [13] Zhu D, Sun C and Qian X. MST1 suppresses viability and promotes apoptosis of glioma cells via upregulating SIRT6 expression. J Integr Neurosci 2019; 18: 117-126.
- [14] Chao Y, Wang Y, Liu X, Ma P, Shi Y, Gao J, Shi Q, Hu J, Yu R and Zhou X. Mst1 regulates glioma cell proliferation via the AKT/mTOR signaling pathway. J Neurooncol 2015; 121: 279-288.
- [15] Dong W, Li L, Teng X, Yang X, Si S and Chai J. End processing factor APLF promotes NHEJ efficiency and contributes to TMZ- and ionizing radiation-resistance in glioblastoma cells. Onco Targets Ther 2020; 13: 10593-10605.
- [16] Lai C, Zhang J, Tan Z, Shen LF, Zhou RR and Zhang YY. Maf1 suppression of ATF5-dependent mitochondrial unfolded protein response contributes to rapamycin-induced radio-sensitivity in lung cancer cell line A549. Aging (Albany NY) 2021; 13: 7300-7313.
- [17] Hill MA. Radiation damage to DNA: the importance of track structure. Radiat Meas 1999; 31: 15-23.
- [18] Cui J, Zhou Z, Yang H, Jiao F, Li N, Gao Y, Wang L, Chen J and Quan M. MST1 suppresses pancreatic cancer progression via ROS-induced pyroptosis. Mol Cancer Res 2019; 17: 1316-1325.
- [19] Zhou T, Chang L, Luo Y, Zhou Y and Zhang J. Mst1 inhibition attenuates non-alcoholic fatty liver disease via reversing Parkin-related mitophagy. Redox Biol 2019; 21: 101120.

- [20] Weng L, Wu Z, Zheng W, Meng H, Han L, Wang S, Yuan Z and Xu Y. Malibatol A enhances alternative activation of microglia by inhibiting phosphorylation of Mammalian Ste20-like kinase1 in OGD-BV-2 cells. Neurol Res 2016; 38: 342-348.
- [21] Kenny TC and Germain D. mtDNA, metastasis, and the mitochondrial Unfolded Protein Response (UPR(mt)). Front Cell Dev Biol 2017; 5: 37.
- [22] Fiorese CJ, Schulz AM, Lin YF, Rosin N, Pellegrino MW and Haynes CM. The transcription factor ATF5 mediates a mammalian mitochondrial UPR. Curr Biol 2016; 26: 2037-2043.
- [23] Lee SJ, Seo BR, Choi EJ and Koh JY. The role of reciprocal activation of cAbl and Mst1 in the oxidative death of cultured astrocytes. Glia 2014; 62: 639-648.
- [24] Desantis V, Lamanuzzi A and Vacca A. The role of SIRT6 in tumors. Haematologica 2018; 103: 1-4.
- [25] Yun HJ, Yoon JH, Lee JK, Noh KT, Yoon KW, Oh SP, Oh HJ, Chae JS, Hwang SG, Kim EH, Maul GG, Lim DS and Choi EJ. Daxx mediates activation-induced cell death in microglia by triggering MST1 signalling. EMBO J 2011; 30: 2465-2476.
- [26] Yang Z, Xu Y, Xu L, Maccauro G, Rossi B, Chen Y, Li H, Zhang J, Sun H, Yang Y, Xu D and Liu X. Regulation of autophagy via PERK-elF2alpha effectively relieve the radiation myelitis induced by iodine-125. PLoS One 2013; 8: e76819.
- [27] Kong EY, Cheng SH and Yu KN. Induction of autophagy and interleukin 6 secretion in bystander cells: metabolic cooperation for radiation-induced rescue effect? J Radiat Res 2018; 59: 129-140.
- [28] Chaurasia M, Gupta S, Das A, Dwarakanath BS, Simonsen A and Sharma K. Radiation induces EIF2AK3/PERK and ERN1/IRE1 mediated pro-survival autophagy. Autophagy 2019; 15: 1391-1406.
- [29] Li Y, Liu F, Wang Y, Li D, Guo F, Xu L, Zeng Z, Zhong X and Qian K. Rapamycin-induced autophagy sensitizes A549 cells to radiation associated with DNA damage repair inhibition. Thorac Cancer 2016; 7: 379-386.
- [30] Tam SY, Wu VW and Law HK. Influence of autophagy on the efficacy of radiotherapy. Radiat Oncol 2017; 12: 57.